European Review for Medical and Pharmacological Sciences 2022; 26: 7115-7124

Diagnostic performance of quantitative signal intensity measurements on magnetic resonance imaging for distinguishing cerebellopontine angle meningioma from acoustic schwannoma

D.-H. NGUYEN[1,2], T.-D. LE[2,3], D.-M. NGUYEN[2], H.-K. NGUYEN[1], Q.-D. NGO[4], D.-H. DUONG[5], M.-D. NGUYEN[6]

[1]Department of Radiology, Hanoi Medical University, Hanoi, Vietnam
[2]Department of Radiology, Viet Duc Hospital, Hanoi, Vietnam
[3]Department of Radiology, VNU University of Medicine and Pharmacy, Vietnam National University, Hanoi, Vietnam
[4]Department of Radiology, Ha Giang General Hospital, Ha Giang, Vietnam
[5]Department of Neurosurgery, Viet Duc Hospital, Hanoi, Vietnam
[6]Department of Radiology, Pham Ngoc Thach University of Medicine, Ho Chi Minh City, Vietnam

Nguyen Duy Hung and Nguyen Minh Duc contributed equally to this article as co-first authors.

Abstract. – OBJECTIVE: Our study investigated magnetic resonance imaging measurements for differentiating cerebellopontine angle (CPA) meningioma from vestibular schwannoma (VS).

PATIENTS AND METHODS: This retrospective study compared 36 meningioma and 36 VS patients. The tumor volume (V_{tumor}) and peritumor edema index (EI) relationship was analyzed. T2-weighted three-dimensional gradient-echo image signal intensity (T23D) and apparent diffusion coefficient (ADC) differentiation cutoff values were defined. Mann-Whitney U test, independent-samples *t*-test, receiver operating characteristic curve, and Spearman's correlation analyses were applied.

RESULTS: Meningioma had higher V_{tumor} (p=0.009) and EI (p=0.031) values than VS. Meningioma had significantly (p<0.001) lower values than VS for mean ADC (ADC_{mean}: 0.841±0.083×10^{-3} *vs.*1.173±0.190×10^{-3} mm^2/s), minimum ADC (ADC_{min}: 0.716±0.078×10^{-3} *vs.*1.045±0.178×10^{-3} mm^2/s), tumor:white matter ADC ratio (rADC: 1.198±0.19 *vs.* 1.59±0.30), mean T23D ($T23D_{mean}$: 142.91±19.9 *vs.* 218.72±84.73), and tumor:adipose T23D ratio (rT23d: 0.19±0.06 *vs.* 0.30±0.28) Cutoff, sensitivity (Se), and specificity (Sp) values were ADC_{min}, 0.856×10^{-3} mm^2/s (Se: 96.6%, Sp: 100%); ADC_{mean}, 0.963×10^{-3} mm^2/s (Se: 96.6%, Sp: 95.5%); rADC, 1.3189 (Se: 93.1%, Sp: 81.8%), $T23D_{mean}$ (Se: 96.6%, Sp: 100%); rT23D, 0.1951 (Se: 89.7%, Sp: 100%), V_{tumor}, 14828.65 mm^3 (Se: 75.0%, Sp: 66.7%), and EI, 1.1025 (Se: 47.2%, Sp: 100%).

CONCLUSIONS: ADC_{min}, ADC_{mean}, rADC, $T23D_{mean}$, rT23D, V_{tumor}, and EI, effectively discriminated meningioma from VS.

Key Words:
Apparent diffusion coefficient, Cerebellopontine angle, Meningioma, Vestibular schwannoma, Edema index.

Introduction

Cerebellopontine angle (CPA) tumors comprise 6%-10% of all cranial tumors[1]. Vestibular schwannoma (VS) is the most frequently encountered tumor type in this region, followed by meningioma[2,3]. In most cases, contrast-enhanced magnetic resonance imaging (MRI) serves as the gold standard imaging method for identifying CPA tumors. However, the imaging manifestations of these two tumor types on conventional MRI have significant overlap. The preoperational definition of CPA tumors is crucial and can affect the optimal treatment strategy, particularly in terms of surgical planning and prognosis[4,5]. The enlarged translabyrinthine approach is preferable for the treatment of schwannomas, whereas a retrosigmoid approach is recommended for CPA meningiomas, despite a higher remission rate, to maintain auditory function and preserve cranial nerves VII and VIII[4-6].

On conventional MRI, schwannomas and meningiomas generally appear hypo- or isointense in T1-weighted imaging (T1WI)[7,8]. On T2-weighted imaging (T2WI), meningiomas

Corresponding Author: Nguyen Minh Duc, MD; e-mail: bsnguyenminhduc@pnt.edu.vn

frequently show homogeneous isointensity and hyperintense signal patterns, whereas schwannomas generally show heterogeneous hyperintensity due to hemorrhage and necrosis[7,8]. Therefore, differences in signal intensity on T2-weighted three-dimensional gradient-echo image (T23D) due to the presence of intratumoral microcysts may contribute to differentiating schwannomas from meningiomas. In addition, CPA meningiomas are generally located eccentric to the internal auditory canal and exhibit a broad dural base, occasionally presenting with a dural tail[9-11], as opposed to VS, which is frequently centrally located and elongated toward the internal auditory canal[11,12]. In addition to conventional MRI sequences, diffusion-weighted imaging (DWI) can be used to garner information regarding the histological and biological features of brain neoplasms. DWI sequences construct images based on the Brownian motion of water molecules within each tissue voxel[2,5,9,10,13,14]. High intratumoral cellularity, as observed in meningioma, tends to obstruct the free movement of water molecules, which is referred to as restricted diffusion[2,5,9,10,13,14]. Neoplasms with loose cell structures, such as VS, facilitate the free movement of water molecules and, therefore, do not show restricted diffusion[13,14]. The degree of restricted diffusion can be measured using apparent diffusion coefficient (ADC) values obtained from ADC maps[15]. Previous studies have described the advantages of using ADC values to differentiate among various cerebral tumors, such as between low-grade and high-grade gliomas and between high-grade gliomas and metastases[16-18].

In this retrospective study, we investigated the diagnostic capabilities of tumor volume (V_{tumor}), the edema index (EI), ADC values, tumor signal intensity on T23D, the ratio between tumor and adipose tissue on T23D imaging (rT23D), and the ratio between tumor and white matter ADC values (rADC) for differentiating CPA meningioma from VS.

Patients and Methods

Study Population

All methods were carried out in accordance with the Declaration of Helsinki. This retrospective study reviewed 72 patients (including 36 with CPA meningiomas and 36 with schwannomas) who were surgically treated at Viet Duc Hospital, Hanoi, Vietnam, from July 2019 to December 2021. All patients received preoperative MRI with conventional sequences and DWI using the same procedures and protocols. All patients underwent surgical intervention, and diagnoses of CPA meningioma or schwannoma were confirmed by pathology.

The following exclusion criteria were applied: patients with a history of previous surgery or radiation therapy; MRI study without DWI or T23D sequences; or noticeable motion artifacts on ADC maps or T23D images, preventing accurate measurements. The institutional review board of Hanoi Medical University approved our retrospective study (Ref: 2687/QD-DHYHN dated 13 July 2021). Due to the retrospective nature of this study, the requirement for informed consent was waived by institutional review board of Hanoi Medical University.

MRI Technique and Protocol

All patients underwent brain MRI examinations using a 1.5 Tesla (T) scanner system (Avanto, Siemens, Germany, and 1.5 T, Phillips, The Netherlands) or a 3.0 T scanner system (Siemens Magnatom Skyra, Siemens, Germany) with head coils. The same conventional MRI and DWI procedures were performed for each patient. DWI was obtained before the contrast administration. The following conventional MRI protocols were used. Axial T1W spin-echo (SE) sequence: repetition time (TR)/echo time (TE) of 490/8.4 ms; slice thickness (ST): 5 mm; field of view (FOV): 250 × 250 mm; matrix size: 240 × 320. Axial high-resolution T23D (trade name CISS, FIESTA, SPACE) was performed as follows: TR/TE: 5600/264 ms; ST: 0.6 mm; FOV: 200 × 200 mm; matrix size: 240 × 320. Axial and sagittal T2W turbo SE sequence: TR/TE: 4100/100 ms; ST: 5 mm; FOV: 250 × 250 mm; matrix size: 240 × 320. Axial fluid-attenuated inversion recovery sequence: TR/TE: 9000/92 ms; inversion time (IT): 25000 ms. Following the intravenous administration of a single gadolinium dose (1 mg/kg bolus), a contrast-enhanced tri-planar T1W SE sequence was obtained: TR/TE: 390/14 ms; FOV: 200 × 200 m; ST: 1 mm. DWI was obtained in the axial plane using an SE, echo-planar imaging sequence: TR/TE: 5600/115 ms; FOV: 250 × 250 mm; matrix size: 128 × 128; ST: 5 mm; b values: 0 and 1000 s/mm^2. ADC maps were reconstructed automatically on a post-processing workstation.

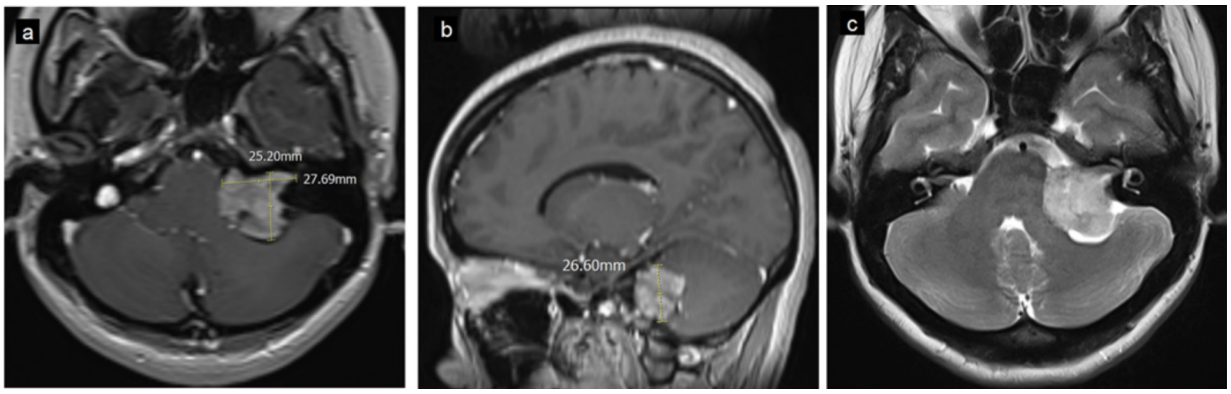

Figure 1. Example of image analysis. A 24-year-old woman with left cerebellopontine angle vestibular schwannoma presented with a heterogeneous and vividly enhanced mass on post-contrast T1-weighted imaging (T1WI) with a minimal extension into the left internal auditory canal (**a**). The three tumor dimensions were measured as maximal diameters on contrast-enhanced T1WI: anterior-posterior diameter and transverse diameter were obtained on axial T1WI image (**a**), and the inferior-superior diameter was obtained on sagittal T1WI (**b**). Tumor volume (V_{tumor}) was 12958.134 mm^3 (calculated using the formula for a spheroid body). The tumor showed mild hyperintensity on axial T2-weighted imaging and no peritumor edema (**c**).

Image Analysis

MRI results were evaluated by a neuroradiologist with more than 10 years of experience who was blinded to the histopathological diagnoses of the patients. Tumor sizes were measured in all three dimensions as the maximal diameter on contrast-enhanced T1WI, including the anterior-posterior diameter (a) and transverse diameter (b) on axial T1WI and the inferior-superior diameter (c) on sagittal T1WI. V_{tumor} was calculated using the formula for spheroid bodies as (19) V_{tumor} = . The combined volume of the tumor and peritumoral brain edema (19) $V_{(tumor + edema)}$ was calculated using the same formula based on dimensions measured on T2WI. The relationship between V_{tumor} and peritumoral brain edema was analyzed using the formula EI = $V_{(tumor + edema)}/V_{tumor}$ (Figure 1).

The following regions were defined:

1. Solid tumor was defined as all tumor regions showing enhancement on contrast enhanced T1WI.
2. Normal contralateral white matter brain parenchyma was the area of white matter with normal signal intensities in all sequences (slightly hyperintense on T1WI, hypointense on T2WI) without mass effect.
3. Hemorrhage or calcified regions were defined as areas with hypointensity on T2* or susceptibility-weighted imaging or hyperdensity on computed tomography (CT).
4. Occipital subcutaneous adipose tissue was defined as hyperintense areas on both T1WI andT2WI.

Areas containing cystic/necrotic features, hemorrhage, or calcifications were excluded from further analyses. For quantitative signal analysis, the tumor and subcutaneous fat signal intensities on T23D images and ADC measurements for the tumor and the normal contralateral white matter brain parenchyma were calculated on the same image slides. ADC measurements were performed using a Syngo workstation (Siemens, Erlangen, Germany) (Figure 2). The T23D and ADC values were acquired using hand-drawn regions of interest (ROIs) containing solid areas of the tumors on the T23D images and ADC maps. ROIs were strategically placed to avoid hemorrhagic, cystic, and calcified regions using T2W* and cranial CT images as references. The occipital subcutaneous fat signal was acquired using the average score from 3 ROIs, obtained by manually positioning uniform ellipsoid ROIs (5-10 mm^2) within the same T23D image slide (Figure 2). The ADC values for normal contralateral white matter brain parenchyma signal were estimated as the average of 2 ROIs smaller than 5 mm^2 (Figure 2) in the same ADC image slides.

Statistical Analysis

Statistical analysis was performed using Statistical Package for Social Sciences version 20.0 (SPSS version 20.0 SPSS Inc., IBM, Armonk, NY, USA). Each parameter following a normal distribution is presented as the mean ± standard deviation (SD). Parameters without a

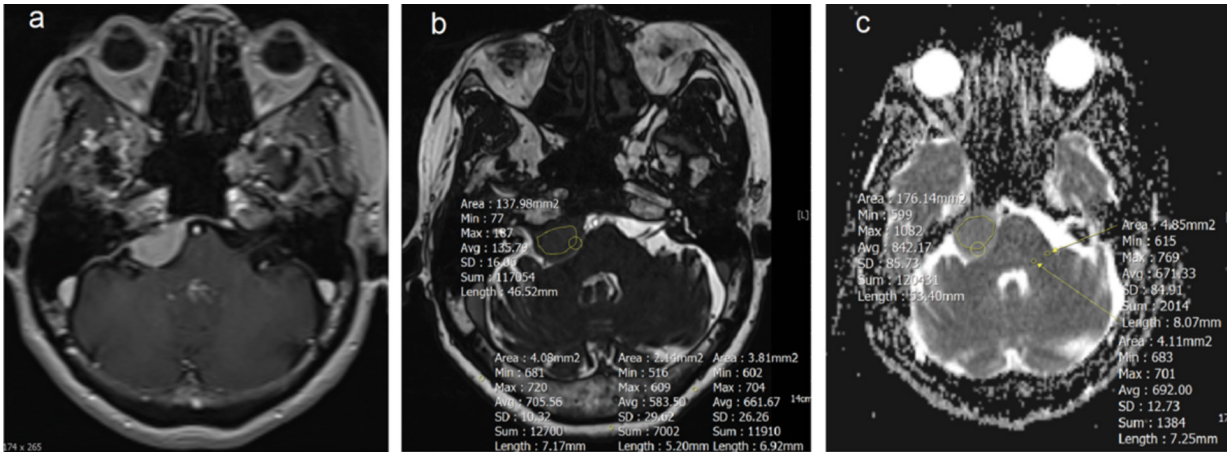

Figure 2. Example of image analysis. A 70-year-old woman with a right cerebellopontine angle meningioma shows homogeneous and vivid enhancement on T1-weighted imaging after contrast administration (**a**). On the high-resolution T2-weighted three-dimensional gradient-echo (T23D) image (**b**), hand-drawn regions of interest (ROIs) were used to identify solid regions of the tumor, and three ROIs were used to measure the signal intensity of occipital subcutaneous fat. On the apparent diffusion coefficient (ADC) map (**c**), hand-drawn ROIs were used to identify solid regions of the tumor, and two ROIs were used to measure contralateral normal white matter signal intensity. $T23D_{mean}$, ADC_{mean}, and ADC_{min} values were calculated from these ROIs for analysis of signal intensity ratios.

normal distribution are presented as the mean and the 25th and 75th percentiles. All variables were assessed for normal distribution using the Shapiro-Wilk test. The Shapiro-Wilk test indicated that the minimum ADC (ADC_{min}), the tumor: subcutaneous fat ratio on T23D (rT23D), EI, and V_{tumor} values followed normal distributions, whereas age, the mean ADC (ADC_{mean}), the tumor:white matter ADC ratio (rADC), and mean T23D ($T23D_{mean}$) values did not follow normal distributions. Therefore, significant differences in ADC_{min}, rT23D, EI, and V_{tumor} were evaluated using the independent-samples *t*-test. The Mann-Whitney U test was used to analyze significant differences in age, ADC_{mean}, rADC, and $T23D_{mean}$ between two independent groups. Relationships between categorical variables were analyzed using the Chi-square test. The correlations between V_{tumor} and peritumor edema values were assessed using Spearman's correlation analysis. To determine the diagnostic capacities of V_{tumor}, EI, ADC values, T23D values, rT23D, and rADC for differentiating between CPA meningioma and VS, receiver operating characteristic (ROC) curve analyses were performed. The cutoff values were determined by maximizing the sum of sensitivity (Se) and specificity (Sp) using the Youden index, and the area under the ROC curve (AUC) was assessed. The *p*-values less than 0.05 were considered significant.

Results

A total of 72 patients were enrolled in this retrospective study (25 men and 47 women), including 36 patients with CPA meningioma and 36 patients with VS. In the meningioma group, 33 cases were histopathology diagnosed as grade I (16 meningothelial, 9 fibrous, 2 angiomatous, and 6 transitional), and 3 were diagnosed as grade II (2 atypical, 1 choroid). The demographic characteristics, V_{tumor}, EI, ADC_{min}, ADC_{mean}, and $T23D_{mean}$ values of the entire cohort are summarized in Table I. No significant differences in sex distribution ($p = 0.768$) or median age ($p = 0.681$) were identified between the two groups. The mean V_{tumor} value was significantly higher in the meningioma group than in the VS group ($p = 0.009$). The EI for the meningioma group was significantly higher than that for the VS group (1.54 *vs.* 1.01; $p = 0.031$). The ADC_{min}, ADC_{mean}, and $T23D_{mean}$ values were significantly lower in CPA meningioma patients than in VS patients ($p < 0.001$ for all).

A strong, positive relationship was identified between V_{tumor} and peritumoral edema in the VS group ($p = 0.001$), whereas no relationship between V_{tumor} and peritumoral edema was identified in the meningioma group ($p = 0.384$) (Table II).

The rT23D and rADC values are presented in Table III. Both rT23D and rADC were significantly lower in CPA meningioma than in VS ($p < 0.001$ for all).

Table I. Demographic characteristics, tumor volumes, peritumor edema index values, ADC_{min}, ADC_{mean}, and $T23D_{mean}$ values according to tumor type.

Parameter	Meningioma group (n = 36)	Schwannoma group (n = 36)	*p*
Sex (F/M)	1/3	4/5	0.768[a]
Age (years)	51.97±13.7	51.08 ± 11.7	0.681[b]
Q1-Q3 (years)	40.5-63	42.5-62	
Range (years)	19-74	24-68	
V_{tumor} (mm^3)	37129.48±35462.84	18380.32±21649.00	0.009[c]
Range (mm^3)	3165.12-150343.20	854-126269.87	
EI	1.54±1.44	1.01±0.03	0.031[c]
Range	1-9.25	1-1.10	
ADC_{mean} ($\times10^{-3}$ mm^2/s)	0.841±0.083	1.173±0.190	< 0.001[b]
Range ($\times10^{-3}$ mm^2/s)	0.707-1061	0.922-1.663	
Q1–Q3 ($\times10^{-3}$ mm^2/s)	0.782-0.884	1.037-1.259	
ADC_{min} ($\times10^{-3}$ mm^2/s)	0.716±0.078	1.045±0.178	< 0.001[c]
Range ($\times10^{-3}$ mm^2/s)	0.577-0.890	0.840-1.590	
$T23D_{mean}$	142.91±19.9	218.72±84.73	< 0.001[b]
Q1-Q3	127.7-156.7	164.5-235.5	
Range	112-188	129-480	

EI: edema index, F: female, M: male; ADC: apparent diffusion coefficient, T23D: high-resolution T2-weighted three-dimensional gradient-echo. Values are given as the mean ± SD; Q1-Q3: the 25th and 75th percentiles of measurements that did not follow normal distributions; *p*: significance level for all pairs; a: Comparisons were performed using the Chi-square test; b: Comparisons were performed using the Mann-Whitney U test, c: Comparisons were performed using the independent-samples *t*-test.

ROC curve analyses were performed to determine the capacity of each parameter to differentiate meningioma from schwannoma, as shown in Figures 3 and 4. The ADC values, consisting of ADC_{mean}, ADCmin, and rADC, had better diagnostic ability to differentiate between schwannoma and meningioma than $T23D_{mean}$, rT23D (Figure 4), V_{tumor}, or EI (Figure 3). The ROC curve analysis results for the discrimination of CPA meningioma from VS groups using V_{tumor}, EI, ADC_{mean}, ADC_{min}, rADC, $T23D_{mean}$, and rT23D are presented in Table IV.

Discussion

Meningioma, with an incidence of 5%-10%, and VS, with an incidence of 80%-90%, are the two most commonly encountered extra-axial tumors in the CPA region[2,3]. The differential diagnosis between these two entities is crucial for optimal surgical planning and prognosis, and studies have suggested that these neoplasms are distinguishable based on differences in radiographic characteristics. MRI is considered the modality of choice compared with CT for the assessment of meningiomas and schwannomas in the CPA region, and MRI assessments may contribute to the evaluation and feature determination of lesions in the posterior cranial fossa[7,11]. On conventional MRI, meningiomas typically present with homogeneous appearances, enhancing vividly on post-contrast sequences with a dural tail sign that occasionally extends into the internal audi-

Table II. Correlation between tumor volume and peritumoral edema according to tumor type.

Parameter	Spearman Correlation	*p* (2-tailed)
Meningioma group (n = 36)	0.150	0.384
Schwannoma group (n = 36)	0.511	0.001

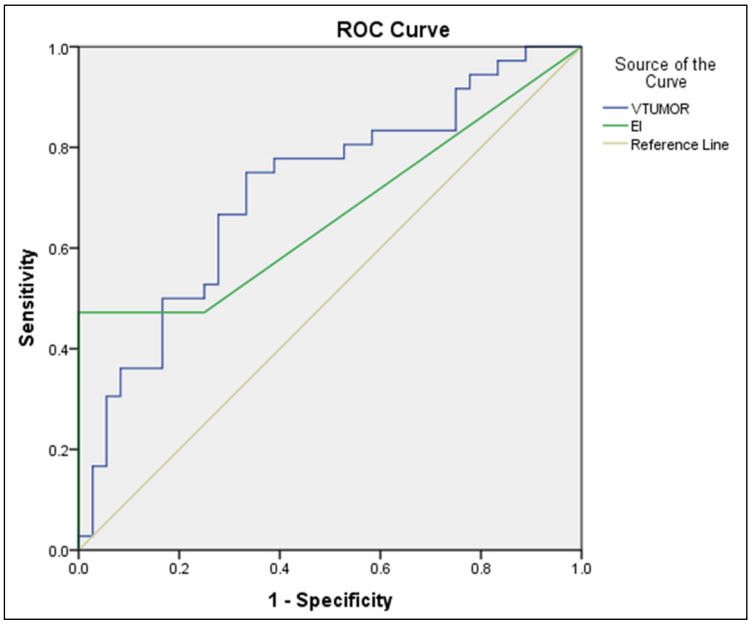

Figure 3. Receiver operating curve (ROC) analysis for edema index (EI) and tumor volume (V_{tumor}) for differentiating cerebellopontine angle meningioma from vestibular schwannoma. The area under the curve values were 0.714 for V_{tumor} and 0.67 for EI.

tory meatus without distending the canal[7,9-11]. By contrast, VS typically manifests as an intensely heterogeneously enhancing mass that extends into the internal auditory meatus and can enlarge the internal auditory meatus with continued development[11,12]. However, in some atypical cases, the radiographic findings of these two tumor types can present with overlapping features that significantly reduce the discrimination ability of MRI in clinical settings, making conventional MR imaging unreliable for the differentiation of meningiomas from schwannomas. Previous studies have reported that approximately 25% of meningiomas had been misdiagnosed as schwannomas[6]. This study attempted to evaluate the usefulness of V_{tumor}, EI, ADC_{mean}, ADC_{min}, $T23D_{mean}$, rADC, and rT23D for differentiating between CPA meningioma and VS.

The tumor volumes of the meningioma group in our study were significantly higher than those of the schwannoma group, with the mean V_{tumor} values of 37129.48 mm^3 and 18380.32 mm^3, respectively (p = 0.009). Our work indicated that a cutoff value for V_{tumor} of 14828.65 mm^3 could distinguish between these two tumor types with Se of 75% and an Sp of 66%. Consistent with previous reports, the mean diameter of meningioma in our cohort was significantly larger than that of VS (13). The research of Bečulić et al[19] concluded that the mean V_{tumor} of meningioma was 2781 ± 2865 cm^3, whereas the mean V_{tumor} for VS was reported as 1747 ± 12.92 mm^3 by Giordano et al[20].

Table III. Signal intensity ratios on T23D (rT23D) and ADC (rADC) according to tumor type.

Parameter	Meningioma group (n = 36)	Schwannoma group (n = 36)	*P*
rT23D	0.19 ± 0.06	0.30 ± 0.28	< 0.001[a]
Range	0.09-0.34	0.17-0.60	
rADC	1.198 ± 0.19	1.59 ± 0.30	< 0.001[b]
Range	0.9-1.87	1.21-2.43	
Q1-Q3	1.05-1.27	1.38-1.71	

AD: apparent diffusion coefficient; T23D: high-resolution T2-weighted three-dimensional gradient-echo; rADC: ratio of tumor to white matter signal intensity on ADC; rT23D: ratio of tumor to subcutaneous adipose tissue signal intensity on T23D. Values are presented as the mean ± SD; Q1-Q3: the 25th and 75th percentiles of measurements that did not follow a normal distribution; p: significance level for all pairs; a: Comparisons were performed using the independent-samples *t*-test; b: Comparisons were performed using the Mann-Whitney U test.

A recent study by Bozdağ et al[13] determined that the maximum diameters of CPA meningioma and VS were 37.18 ± 14.55 mm and 27.35 ± 9.22 mm, respectively.

In our study, the EI value for meningioma (1.54) was significantly higher than that for schwannoma (1.01; p = 0.031). The EI value ranged from 1 to 9.25 in the meningioma group and from 1 to 1.10 in the schwannoma group. Our results do not fully correspond with prior investigations. Bečulić et al[19], in a publication examining peritumoral edema in meningiomas, reported a mean EI value of 4.87 ± 4.19, ranging from 1 to 14, and a study by You et al[21] reported a mean EI value for schwannoma of 1.53 ± 0.22. Our research revealed no significant linear correlation between EI and V_{tumor} (using Spearman's correlation analysis) in meningioma, but a strong correlation was observed between V_{tumor} and EI in schwannoma (p = 0.001). These results were similar to those reported in previous studies[20,21]. In our analysis, both V_{tumor} and EI values for schwannoma were significantly lower than those for meningioma, with an EI cutoff of 1.1025 discriminating between these two tumor types with a Se of 47.2% and an Sp of 100%. The low value obtained for Se may be due to the inconsistent appearance of peritumoral edema in the meningioma group and the lack of any significant linear correlation between EI and V_{tumor} in meningioma. A recent study highlighted the relationship between the expression levels of vascular endothelial growth factor and the EI value in schwannoma, suggesting the necessity of developing new effective treatments to alleviate symptoms and reduce postoperative complications[21]. Prior research yielded correlations between the EI value and a series of factors, including tumor volume, the tumoral margin and invasion (based on intraoperative evaluation), and the Ki-67 value[19].

Additionally, the signal intensities measured for solid components on the ADC map may help in differentiating between schwannomas and meningiomas. In this study, the ADC_{mean} and ADC_{min} values for schwannoma were markedly higher than those for meningioma ($p < 0.001$), which is similar to previous findings[13,14,16]. The ADC_{mean} values for meningiomas and schwannomas were 0.841 ± 0.083 × 10^{-3} mm^2/s and 1.173 ± 0.190 × 10^{-3} mm^2/s, respectively. The ADC_{min} values for meningioma and schwannoma were 0.716 ± 0.078 × 10^{-3} mm^2/s and 1.045 ± 0.178 × 10^{-3} mm^2/s, respectively. We hypothesize that the high cellularity features associated with a sizable nuclear-cytoplasmic ratio in meningioma may contribute to these low ADC values on diffusion images[13,14,16,17]. Schwannomas, by comparison, consist of Antoni A and B cells. Antoni B cells often feature loose stroma and cell structures, leading to intratumoral cystic patterns, whereas Antoni A cells are responsible for dense tumor regions. This heterogeneous tumoral structure in

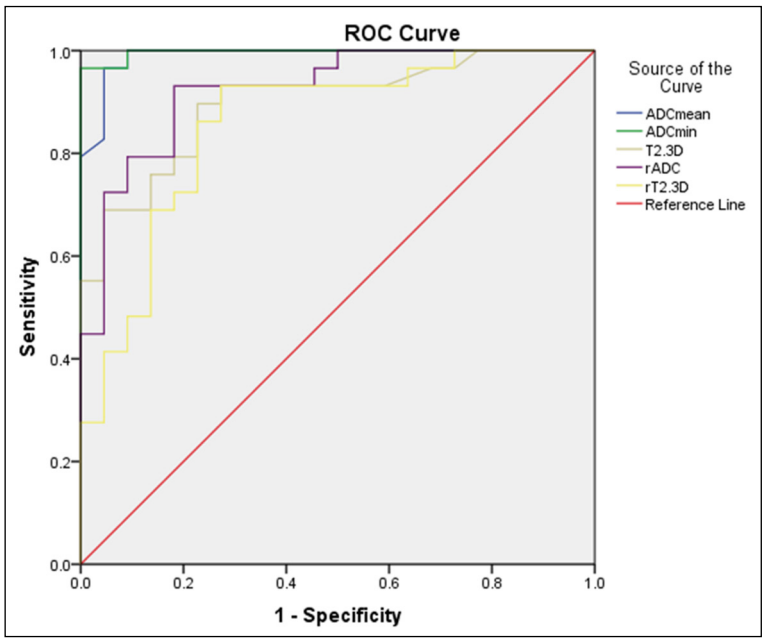

Figure 4. Receiver operating characteristic (ROC) curve analysis the abilities of the following parameters to discriminate between cerebellopontine angle (CPA) meningioma from vestibular schwannoma: mean (ADC_{mean}) and minimum (ADC_{mni}) tumor values on apparent diffusion coefficient (ADC), tumor to white matter signal intensity ratio on ADC (rADC), mean value on high-resolution T2-weighted three-dimensional gradient-echo ($T23D_{mean}$), and ratio of tumor to subcutaneous adipose signal intensity on T23D (rT23D). Area under the curve values were as follows: ADC_{mean} = 0.990; ADC_{min} = 0.997; $T23D_{mean}$ = 0.897; rADC = 0.923; and rT23D = 0.856.

Table IV. The ROC parameters for discriminating CPA meningioma from VS.

Parameter	AUC	Cutoff	Sensitivity	Specificity	Youden
V_{tumor} (mm^3)	0.714	14828.65	75.0	66.7	0.417
EI	0.67	1.1025	47.2	100	0.472
ADC_{mean} ($\times 10^{-3}$ mm^2/s)	0.990	0.963	96.6	95.5	0.920
ADC_{min} ($\times 10^{-3}$ mm^2/s)	0.997	0.856	96.6	100	0.966
$T23D_{mean}$	0.897	155.5	89.7	77.3	0.669
rADC	0.923	1.3189	93.1	81.8	0.749
rT23D	0.856	0.1951	93.1	72.7	0.658

ROC: receiver operating characteristic; ADC: apparent diffusion coefficient; AUC: area under the ROC curve, rADC: tumor to white matter signal intensity ratio in ADC; rT23D: tumor to subcutaneous adipose tissue signal intensity ratio in T23D; CPA: cerebellopontine angle; VS: vestibular schwannoma.

VS allows for the free movement of water molecules in the extracellular space, resulting in a higher ADC value for schwannomas, despite the presence of solid component areas[17,22].

The rADC value for meningioma was significantly lower than that for schwannoma in our research ($p < 0.001$). The rADC value of meningioma was 1.198 ± 0.19, whereas the rADC value of schwannoma was 1.59 ± 0.30. The findings reported by Pavlica et al[14] comparing the tumor to contralateral normal parenchyma signal intensity ratios between CPA meningioma and VS corresponded with our results. Additionally, the ADC values recorded for the normal white matter in our patients were in line with the results reported by previous studies[17,18].

The mean signal intensity on T23D and the rT23D values for meningioma (142.91 ± 19.9 and 0.19 ± 0.06, respectively) were significantly lower than those for schwannoma (218.72 ± 84.73 and 0.30 ± 0.28, respectively). No previous research has reported on the usefulness of signal intensities from T23D or rT23D; however, we speculate that these findings may be associated with divergent tumoral structures between these two neoplasms, which is supported by differences in the signal intensities on the ADC map. Meningiomas generally feature high cellularity and rarely contain cystic components, which manifest as low signal intensity on T2WI[9,10,22]. By comparison, small schwannomas often demonstrate homogeneous appearances due to the predominance of Antoni A cells, whereas larger VS entities often exhibit high signal intensity on T2WI and heterogeneous post-contrast enhancement, indicating the presence of cystic components, necrosis, and microcystic areas, likely due to an increased proportion of Antoni B cells[22].

According to ROC analyses, the ADC_{min} value (AUC: 0.997) provided the best differential diagnostic performance, followed by ADC_{mean}, rADC, $T23D_{mean}$, and rT23D (AUC values of 0.990, 0.923, 0.897, and 0.856, respectively). Significant differences in ADC_{mean} and ADC_{min} between these two entities have been reported in several prior studies[13,14,16]. In our literature search, both Bozdağ et al[13] and Pavlisa et al[14] concluded that no overlap existed between schwannomas and meningiomas when comparing ADC_{mean} and ADC_{min} values. The cutoff values recommended by Bozdağ et al[13] were 1.027 $\times 10^{-3}$ mm^2/s (Se: 92.86%, Sp: 100%) for ADC_{mean} and 0.980 $\times 10^{-3}$ mm^2/s (Se: 92.86%, Sp: 100%) for ADC_{min}. Our cutoff values were lower than these, at 0.963 $\times 10^{-3}$ mm^2/s (Se: 92.86%, Sp: 100%) for ADC_{mean} and 0.856 $\times 10^{-3}$ mm^2/s (Se: 92.86%, Sp: 100%) for ADC_{min}. We believe that differences in the placement of ROIs may have contributed to the divergence between these results. The study by Bozdağ et al[13] obtained tumor signal intensities by placing 5-mm^2 ROIs, whereas our study used hand-drawn ROIs to encompass all of the solid tumoral components. Calcifications, hemorrhages, and necrotic regions were strategically eliminated from further measurements in both studies.

Several limitations are associated with our retrospective study, and we believe that specific issues can be addressed in future studies. First, the number of subjects included in the study was small, and the

study cohort may not represent all ethnic groups. The second limitation is that our data set did not encompass the grade III meningioma group. The disproportionate representation of grade I and II meningiomas in our study cohort might lead to inaccurate results. We believe that further investigations in larger populations, including grade III meningiomas, are warranted to validate the results of this study.

Conclusions

In summary, our data indicate that several diagnostic issues encountered in patients with meningiomas and schwannomas can be circumvented through the use of V_{tumor}, EI, ADC signal intensity values, T23D signal intensity values, rADC, and rT23D. According to our study, ADC_{min} is the most effective parameter for differentiating between meningioma and schwannoma, followed by ADC_{mean}, rADC, $T23D_{mean}$, and rT23D. MRI evaluations can play an essential role in the differential diagnosis of tumor entities with similar presentations, facilitating the correct classification of patients and improving accuracy in the diagnosis and optimization of treatment.

Conflicts of Interest

All authors have completed the ICMJE uniform disclosure form. The authors have no conflicts of interest to declare.

Acknowledgments

None.

Data Availability

The datasets generated and/or analysed during the current study are not publicly available due to privacy concerns but are available from the corresponding author on reasonable request.

Authors' Contributions

D.-H. Nguyen and M.-D. Nguyen contributed equally to this article as first authorship. D.-H. Nguyen and M.-D. Nguyen: designed and conducted research, analysed data, wrote and reviewed paper; D.-H. Nguyen and M.-D. Nguyen: reviewed paper and has primary responsibility for the final version of manuscript. All authors read and approved the manuscript.

Ethical Statement

The authors are accountable for all aspects of the work in ensuring that questions related to the accuracy or integrity of any part of the work are appropriately investigated and resolved. The study was conducted in accordance with the Declaration of Helsinki (as revised in 2013). The institutional review board of Hanoi Medical University approved this retrospective study (Ref: 2687/QD-DHYHN dated 13 July 2021). Due to the retrospective nature of this study, the requirement for informed consent was waived by institutional review board of Hanoi Medical University.

ORCID ID

Nguyen Minh Duc: 0000-0001-5411-1492.

Funding

None.

References

1) Moffat DA, Ballagh RH. Rare tumours of the cerebellopontine angle. Clin Oncol (R Coll Radiol) 1995; 7: 28-41.
2) Chen AF, Samy RN, Gantz BJ. Cerebellopontine angle tumor composed of Schwann and meningeal proliferations. Arch Otolaryngol Head Neck Surg 2001; 127: 1385-1389.
3) Brunori A, Scarano P, Chiappetta F. Non-acoustic neuroma tumor (NANT) of the cerebello-pontine angle: a 15-year experience. J Neurosurg Sci 1997; 41: 159-168.
4) Nakamura M, Roser F, Dormiani M, Matthies C, Vorkapic P, Samii M. Facial and cochlear nerve function after surgery of cerebellopontine angle meningiomas. Neurosurgery 2005; 57: 77-90.
5) Samii M, Matthies C. Management of 1000 vestibular schwannomas (acoustic neuromas): surgical management and results with an emphasis on complications and how to avoid them. Neurosurgery 1997; 40: 11-21.
6) Grey PL, Moffat DA, Hardy DG. Surgical results in unusual cerebellopontine angle tumours. Clin Otolaryngol Allied Sci 1996; 21: 237-243.
7) Imhof H, Henk CB, Dirisamer A, Czerny C, Gstöttner W. CT und MRT tumoröser Veränderungen des Schläfenbeins. Radiologe 2003; 43: 219-226.
8) Singh K, Singh MP, Thukral C, Rao K, Singh K, Singh A. Role of magnetic resonance imaging in evaluation of cerebellopontine angle schwannomas. Indian J Otolaryngol Head Neck Surg 2015; 67: 21-27.
9) Maiuri F, Iaconetta G, de Divitiis O, Cirillo S, Di Salle F, De Caro ML. Intracranial meningiomas: correlations between MR imaging and histology. Eur J Radiol 1999; 31: 69-75.
10) Soyama N, Kuratsu J, Ushio Y. Correlation between magnetic resonance images and histology in meningiomas: T2-weighted images indicate collagen contents in tissues. Neurol Med Chir (Tokyo) 1995; 35: 438-441.

11) Lalwani AK, Jackler RK. Preoperative differentiation between meningioma of the cerebellopontine angle and acoustic neuroma using MRI. Otolaryngol Head Neck Surg 1993; 109: 88-95.

12) Bonneville F, Savatovsky J, Chiras J. Imaging of cerebellopontine angle lesions: an update. Part 1: enhancing extra-axial lesions. Eur Radiol 2007; 17: 2472-2482.

13) Bozdağ M, Er A, Ekmekçi S. Diagnostic Efficacy of Signal Intensity Ratio and Apparent Diffusion Coefficient Measurements in Differentiating Cerebellopontine Angle Meningioma and Schwannoma. Erciyes Med J 2020; 42: 281-288.

14) Pavlisa G, Rados M, Pazanin L, Padovan RS, Ozretic D, Pavlisa G. Characteristics of typical and atypical meningiomas on ADC maps with respect to schwannomas. Clin Imaging 2008; 32: 22-27.

15) Chen L, Liu M, Bao J, Xia Y, Zhang J, Zhang L, Huang X, Wang J. The correlation between apparent diffusion coefficient and tumor cellularity in patients: a meta-analysis. PLoS One 2013; 8: e79008.

16) Yamasaki F, Kurisu K, Satoh K, Arita K, Sugiyama K, Ohtaki M, Takaba J, Tominaga A, Hanaya R, Yoshioka H, Hama S, Ito Y, Kajiwara Y, Yahara K, Saito T, Thohar MA. Apparent diffusion coefficient of human brain tumors at MR imaging. Radiology 2005; 235: 985-991.

17) Sener RN. Diffusion MRI: apparent diffusion coefficient (ADC) values in the normal brain and a classification of brain disorders based on ADC values. Comput Med Imaging Graph 2001; 25: 299-326.

18) Hakyemez B, Yildirim N, Gokalp G, Erdogan C, Parlak M. The contribution of diffusion-weighted MR imaging to distinguishing typical from atypical meningiomas. Neuroradiology 2006; 48: 513-520.

19) Bečulić H, Skomorac R, Jusić A, Alić F, Mašović A, Burazerović E, Omerhodžić I, Dorić M, Imamović M, Mekić-Abazović A, Efendić A, Udovčić-Gagula D. Correlation of peritumoral brain edema with morphological characteristics and ki67 proliferative index in resected intracranial meningiomas. Acta Clin Croat 2019; 58: 42-49.

20) Giordano M, Gerganov V, Metwali H, Gallieni M, Samii M, Samii A. Imaging features and classification of peritumoral edema in vestibular schwannoma. Neuroradiol J 2020; 33: 169-173.

21) You HH, Chen XY, Chen JY, Bai Y, Chen FX. The Relationship Between Peritumoral Brain Edema and the Expression of Vascular Endothelial Growth Factor in Vestibular Schwannoma. Front Neurol 2021; 12: 691378.

22) Gomez-Brouchet A, Delisle MB, Cognard C, Bonafe A, Charlet JP, Deguine O, Fraysse B. Vestibular schwannomas: correlations between magnetic resonance imaging and histopathologic appearance. Otol Neurotol 2001; 22: 79-86.